2021

Simulations of Forces for Total Knee Arthroplasty

JOURNAL OF ADVANCED BIOMECHANICS, VOLUME 531

KENNY MILLER

Table of Contents

Abstract

Introduction

Since medical professionals have been replacing knees for patients, the question has been how we can best replicate the human knee to reduce patient pain and improve the use of their implant. Total Knee Arthroplasties (TKAs) have generally had success in the past with lifespans approximately 15 years and strong survival-rates. Concerns during TKA stem from any similar surgery but there are also specific cases with TKA that include patellar tracking and condylar rollback. Surgeons and implant designers have been trying to improve these for better patient outcomes.

Methods

This study utilizes software, Autolev, to generate a theoretical model for the posterior cruciate retaining implant utilized by our surgeon in this patient's TKA. The software then takes the model and generates a simulation to which this study passes measurements from CT and MRI scans of the patient to segment relevant patient specific geometries and attachment sites. This allows for a more focused analysis for this patient and implant performance. The final simulation utilizes all the model code to reproduce our patient's deep knee bend activity to analyze the forces experienced. The model was run both with and without muscle wrapping for the four sub-components of the quadriceps muscle.

Results

In this study it was found that the implant used for the patient was most accurately measured when muscle wrapping was included in the model. The patient experienced quadricep forces that peaked at 4.5x BW and patellar tendon forces that peaked at 3x BW with this implant. The peaks typically occurred around 80-90 degrees of knee flexion. The patient also saw torques on the bone consistent with what is to be expected. The implant showed promise at reducing the torques on the bone around 80 degrees of flexion when it separates (not continuous) for the femur and patella.

Discussion

This study shows promise for the PCR implant utilized in this TKA. The patient saw more consistent forces and torque on their bone and muscles with the implant and muscle wrapping. The simulation shows better patellar tracking and condylar rollback when we review the contact points and torques throughout the activity. This implant appears to be promising for future TKAs but further analysis with a larger patient base is needed before any impending decisions can be prepared and conclusions drawn.

Introduction

Total Knee Arthroplasty (TKA) is also typically called knee replacement surgery. The focus on a TKA is to help relieve pain and restore function to severely diseased or injured knee joints. This procedure involves cutting away damaged bone and cartilage from the tibia, femur, and patella and replacing it with an implant (Mayo Clinic, 2021). TKAs have a positive success rate (survival rate of the implanted prosthesis), in a study from September 1990 to June 2009 it was found that TKAs in 194 patients had 97.2%, 91.6% and 86.1% survival rates at 5-, 8-, and 10-year intervals, respectively (Bae, et. al, 2012).

While TKAs have had positive success, they do carry risks like any surgery. There are risks of infection, clotting and subsequent heart attack/stroke, or nerve damage. While these risks are important to note they are not the norm. The main problem associated with a TKA is the life of the implant. Knee replacements can wear out and usually last about 15 years (Mayo Clinic, 2021). Bernardo Innocenti, et. al 2011, found that patella-femoral and tibio-femoral contact forces can alter depending on the implant design; this is another concern of TKAs is how to develop an implant to better address each individual patient. One additional concern of the TKAs is regarding patellar tracking, it has been found that mobile platform TKA significantly improve patellar tracking and decreased the patellofemoral contact stress (Saqaguchi, et. al, 2009). There is also considerable concern about condylar rollback, where Massing and Gournay (2005) studied how different offsets during surgery could alter knee flexion impingement. To address these concerns most companies are attempting to improve the implant by reducing patient pain levels, providing patients with better function in their daily lives and sports/recreation. To do this they are focused on adjustments to the designs and implementation of their implants in surgery.

Theoretical modeling will be utilized in this paper. It will be utilized to represent the implant within the patient's left knee and how it is working. The benefits of theoretical modeling are that we can imitate the implant and study it without having to work on the patient after data collection and we can recommend future adjustments to better suit patients going forward. This form of modeling will allow us to gain insights into the forces acting on the patient's implant when performing deep knee bend activities and provides the opportunity to study them after the implant is placed into the individual.

The objective of this study is to model the implanted TKA on a patient's left knee and estimate the forces acting on the implant. The chosen implant for this patient is a fixed bearing PCR (posterior cruciate retaining) implant, which will resect the patient's ACL but retain the PCL.

Methods

The model for this study was developed utilizing the software Autolev. Autolev is used for symbolic manipulation for motion analysis. By inputting bodies into the software, this study was able to model the foot, femur, tibia, patella, and pelvis as well as the PCL, MCL, and LCL ligaments and sub-components of the quadriceps.

The bone representation was developed with the bodies in mind. Each bone was assigned an individual reference frame and contact points to the ground (foot) or other bodies. The bones are then passed throughout the software as bodies that are changing position over time.

The ligaments are modeled in a similar fashion to the bones. There are connection points on the respective bones (bodies) in the patient. The ligaments are then modeled like a spring. The study uses the slack length, stiffness, strain, and current length of the ligament to model the forces acting on the ligaments.

The four sub-components of the quadriceps muscle, the rectus femoris, vastus lateralis, vastus medialis, and vastus intermedius, and patellar tendon are the muscles modeled by this study. They are modeled using connection points on the bones specified in the modeling software. The software uses reference points to simulate and measure the forces acting on the muscles.

To ensure proper representation of the kinematics of our patient 3rd-order polynomials were fit for measurements collected from CT and MRI scans of the patient. The polynomials were fit based on data collected over two second intervals from 0 to 9.2 seconds. The terms fit include angle inputs/changes of the tibia, femur, pelvis, and patella. This study also fit force plate data to determine how ground reaction forces changed over time. Finally, changes in reference points between the bodies were input as polynomials too.

Results

The models developed for this study include one without quadriceps muscle wrapping. The model without wrapping shows a significant spike of the forces exerted by the quadricep in extension activities due to this; when the model is corrected to include wrapping the study shows more accurate forces on the respective muscles and ligaments.

The simulation developed showcases the forces and torques experienced by the patient's knee. The forces appear to be reasonable peaking around 4.5x BW for the quadriceps when wrapping is taken into effect (Figure 12) instead of spiking around 7x BW (Figure 1). With the patellar ligament peaking at about 3x BW for the force it experiences (Figure 12). The forces experienced by the body all peak around 90 degrees of knee flexion (Figures 12-14). The main changes, other than reasonable forces, in the kinetics for these two models is in the torques on the body. The torques for the patella and femur are not continuous (Figures 16 & 17), separating at 80 degrees.

The simulation also showed how the contact points alter throughout the deep knee bend activity. The study sees that the patient experiences smooth transitions throughout the activity (Figures 21 & 22) and moves smoothly with regards to the angles of the body's components (Figure 20). There are not significant changes in the resulting plots of the simulation without muscle wrapping versus the simulation with wrapping of the quadriceps.

Discussion

This study found the implant chosen for this patient yielded strong outcomes for the specific patient tested. The implant's performance when modeled with quadriceps wrapping shows significantly better results than the simulation without wrapping. The implant also shows promise in maintaining

pre-surgical levels of rollback. We see in Figures 16 and 17 where the femur has a drop in its torque as the flexion continues deeper. In those same figures we see the patella, and in turn patellar tracking, also shift at 80 degrees and improve. The torques experienced on the bones in this simulation are within general values of less than or close to 100 N-m. The implant appears to do a fine job in supporting the patient's motion and the forces exerted while completing a deep knee bend activity.

In the process of generating this model/simulation the following assumptions were made:

- The foot, tibia, femur, patella, and pelvis are bodies with mass and moment of inertia
- The implant components are rigidly fixed to their corresponding bodies
- The ankle and hip joints are fixed helical/spherical joints
- There are two variable contact points for the femorotibial articulation
- There is one contact point between the patellofemoral articulation
- The ratio of forces generated by the four sub-components of the quadriceps muscle are equal to the ratio of the physiological cross-sectional area (PCSA) of the sub-components:
    - All values for the PCSA were collected from a study completed by Erskine, et. al. (2009)
        - Rectus Femoris: 49.8/225.8 = ~ 0.22
        - Vastus Lateralis: 75.1/225.8 = ~0.33
        - Vastus Medialis: 44.4/225.8 = ~0.20
        - Vastus Intermedius: 56.5/225.8 = 0.25

This model is not without its limitations. The simulation does not have multiple patients to confirm any results from this patient, while the implant appears promising we do not have data on other cases to confirm. The simulation does not have data on the patient both pre- and post-operative to compare how the implant is performing compared to a patient baseline.

References

Bae DK, Song SJ, Heo DB, Lee SH, Song WJ. Long-term survival rate of implants and modes of failure after revision total knee arthroplasty by a single surgeon. J Arthroplasty. 2013 Aug;28(7):1130-4. doi: 10.1016/j.arth.2012.08.021. Epub 2012 Dec 7. PMID: 23219625.

Erskine, Robert & Jones, David & Maganaris, Constantinos & Degens, Hans. (2009). In vivo specific tension of the human quadriceps femoris muscle. European journal of applied physiology. 106. 827-38. 10.1007/s00421-009-1085-7.

Innocenti B, Pianigiani S, Labey L, Victor J, Bellemans J. Contact forces in several TKA designs during squatting: A numerical sensitivity analysis. J Biomech. 2011 May 17;44(8):1573-81. doi: 10.1016/j.jbiomech.2011.02.081. Epub 2011 Mar 23. PMID: 21435645.

Massin P, Gournay A. Optimization of the posterior condylar offset, tibial slope, and condylar roll-back in total knee arthroplasty. J Arthroplasty. 2006 Sep;21(6):889-96. doi: 10.1016/j.arth.2005.10.019. PMID: 16950045.

Mayo Clinic. "Knee Replacement." *Mayo Clinic*, Mayo Foundation for Medical Education and Research, 18 Aug. 2021, https://www.mayoclinic.org/tests-procedures/knee-replacement/about/pac-20385276.

Sawaguchi N, Majima T, Ishigaki T, Mori N, Terashima T, Minami A. Mobile-bearing total knee arthroplasty improves patellar tracking and patellofemoral contact stress: in vivo measurements in the same patients. J Arthroplasty. 2010 Sep;25(6):920-5. doi: 10.1016/j.arth.2009.07.024. Epub 2009 Sep 23. PMID: 19775856.

Appendix

Model Without Wrapping Figures

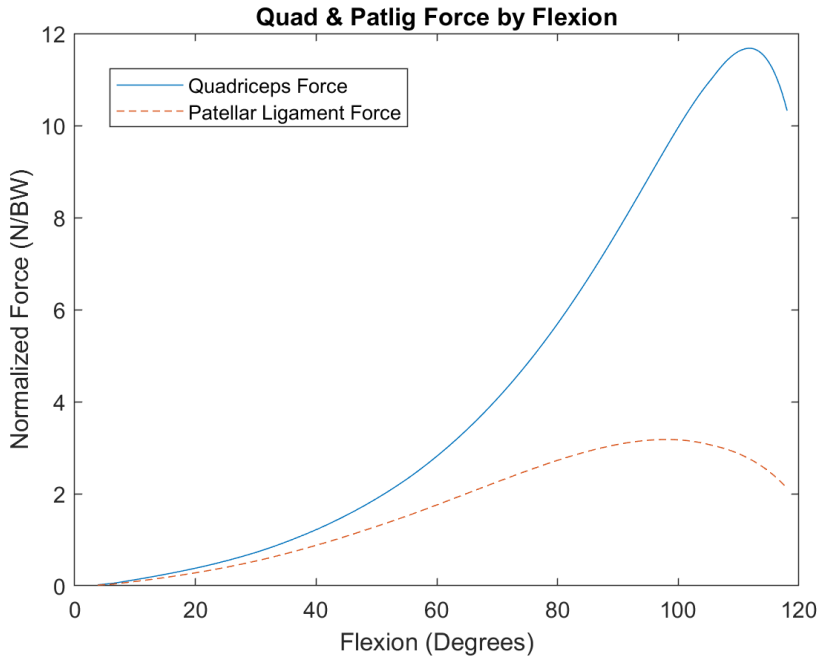

Figure 1: Plot showing the total quadriceps force and patellar ligament force

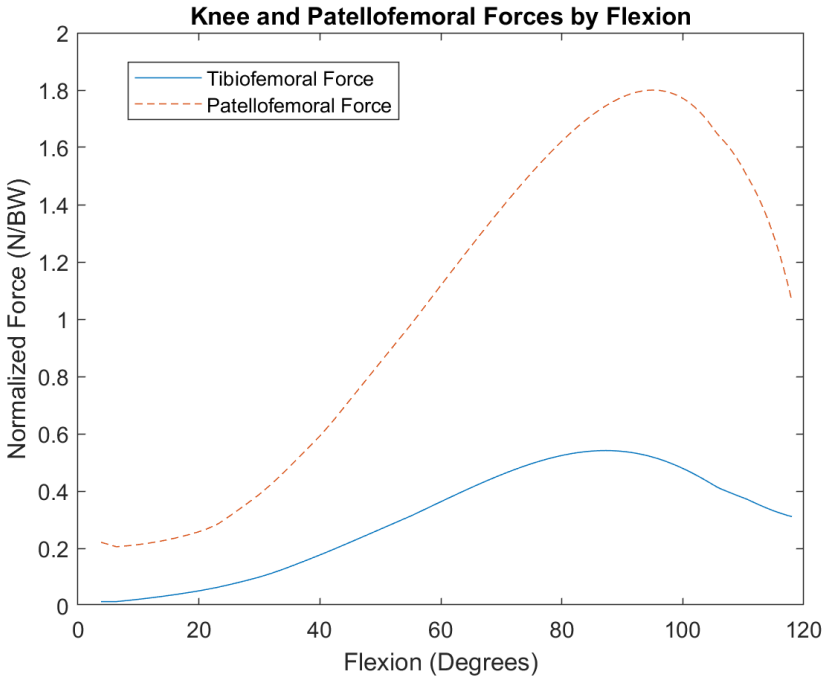

Figure 2: Plot showing the resultant tibiofemoral (knee) and patellofemoral forces

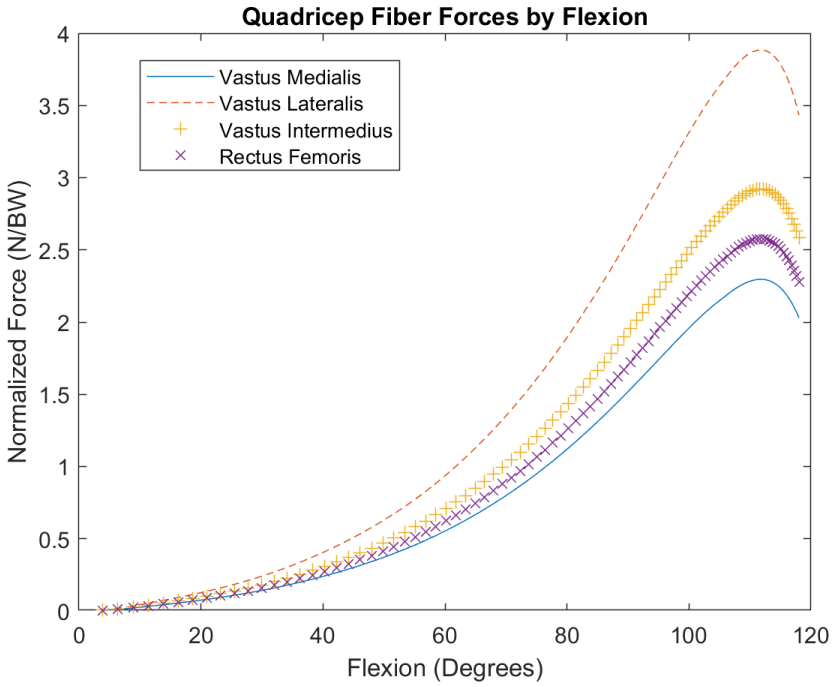

Figure 3: Plot showing the separate force in each quadriceps muscle fiber.

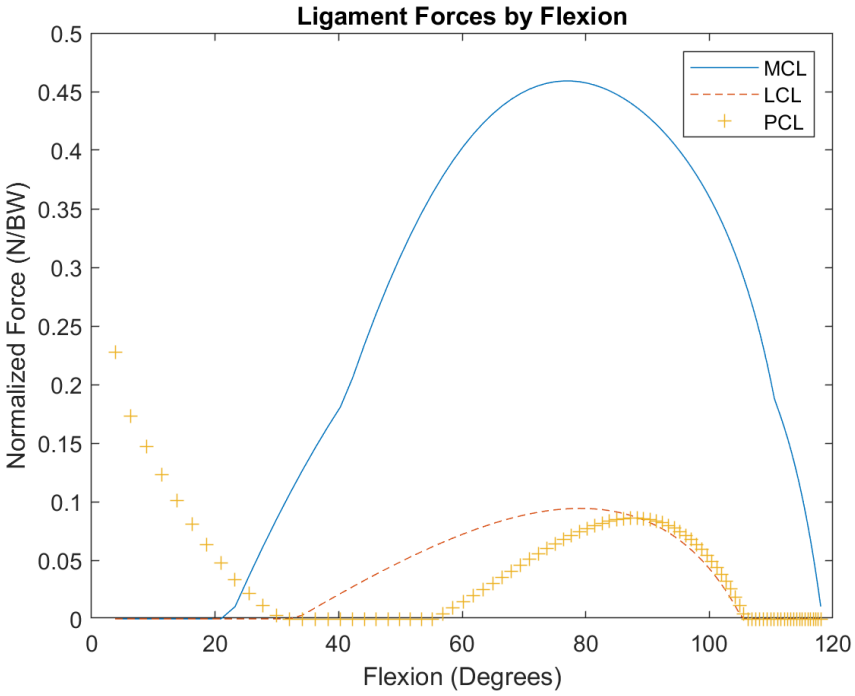

Figure 4: Plot showing the total MCL, LCL, and PCL ligament forces

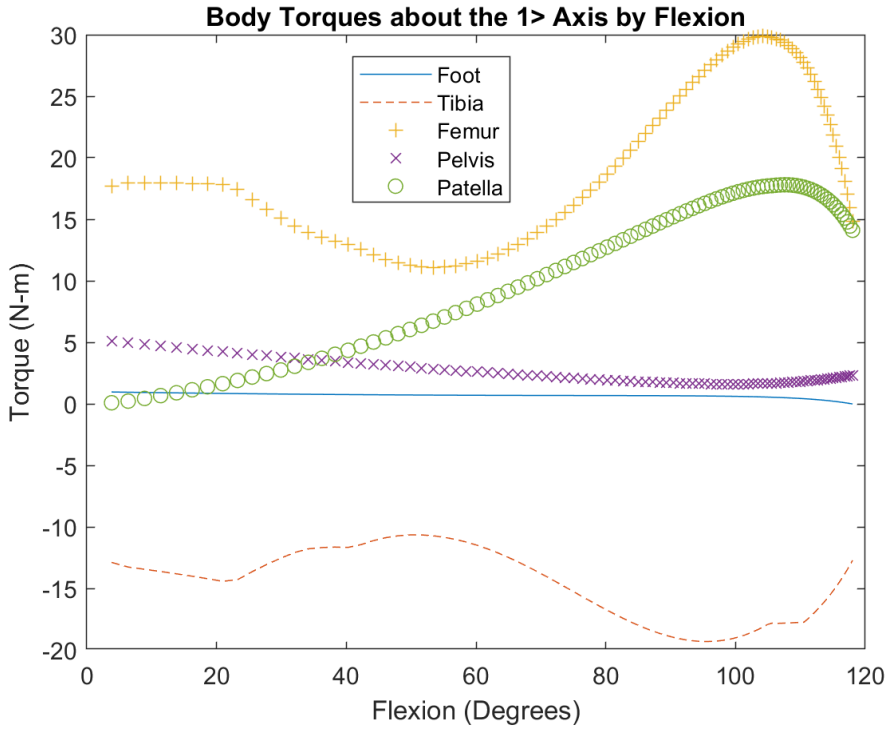

Figure 5: Plot showing the torques on the foot, tibia, femur, pelvis, and patella about the 1> axis

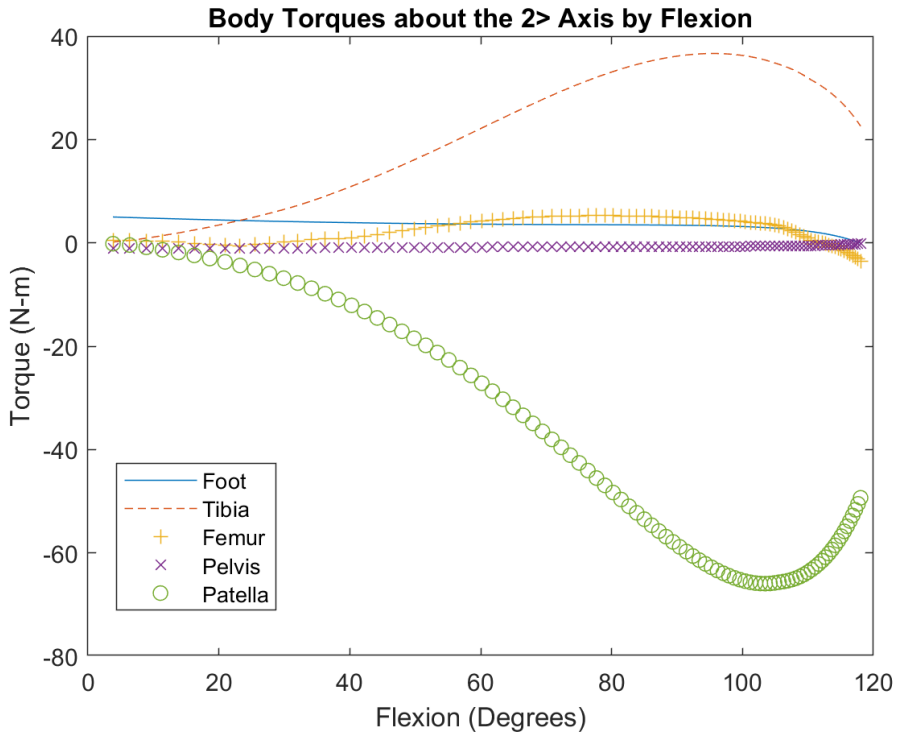

Figure 6: Plot showing the torques on the foot, tibia, femur, pelvis, and patella about the 2> axis

Figure 7: Plot showing the torques on the foot, tibia, femur, pelvis, and patella about the 3> axis

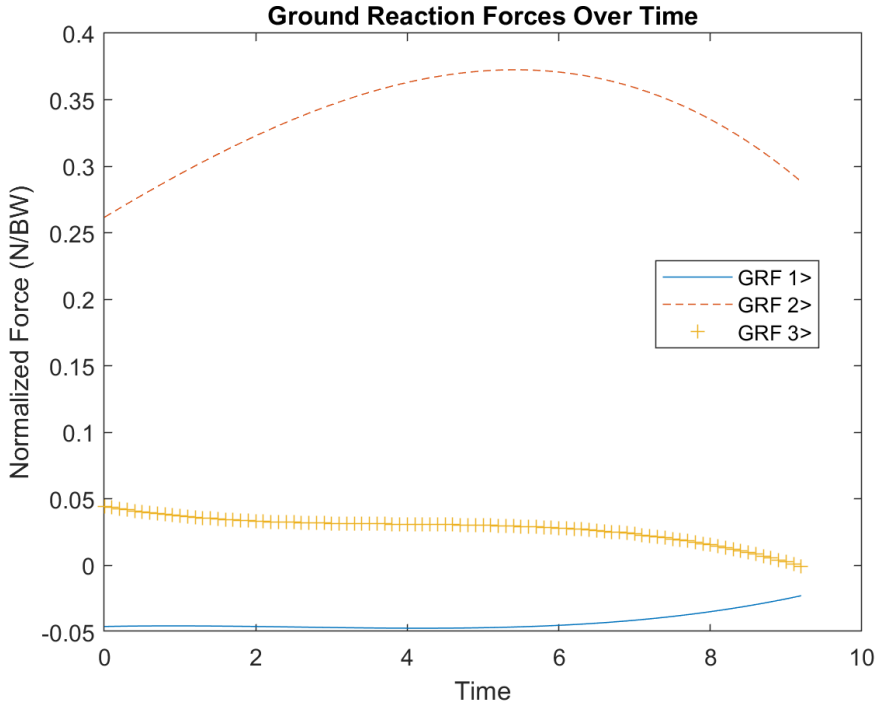

Figure 8: Plot showing the GRF forces in the 1>, 2>, and 3> direction

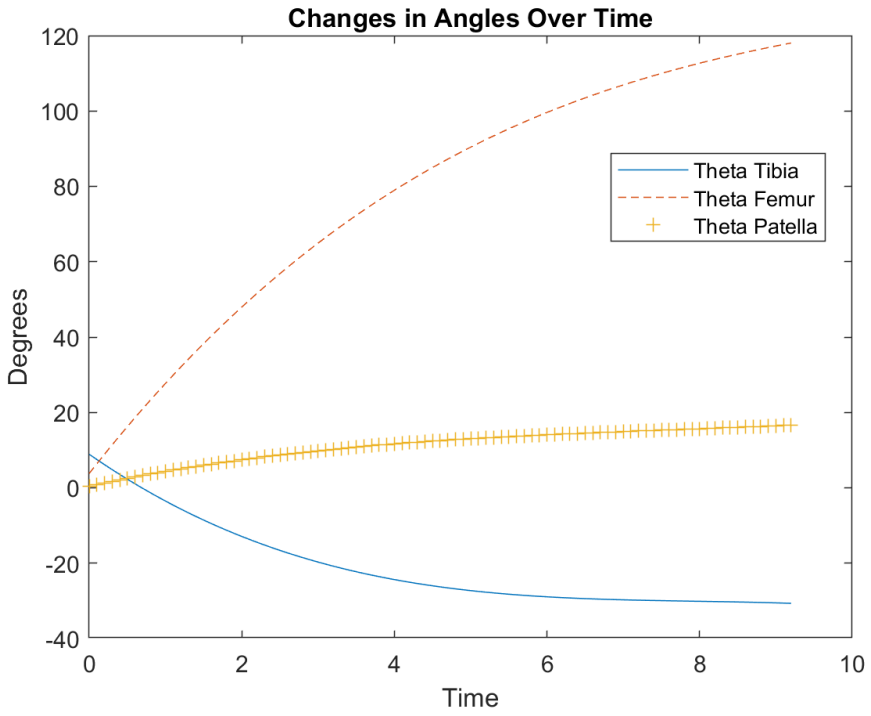

Figure 9: Plot showing theta tibia, theta femur about 3> axis , and theta patella about 3> axis

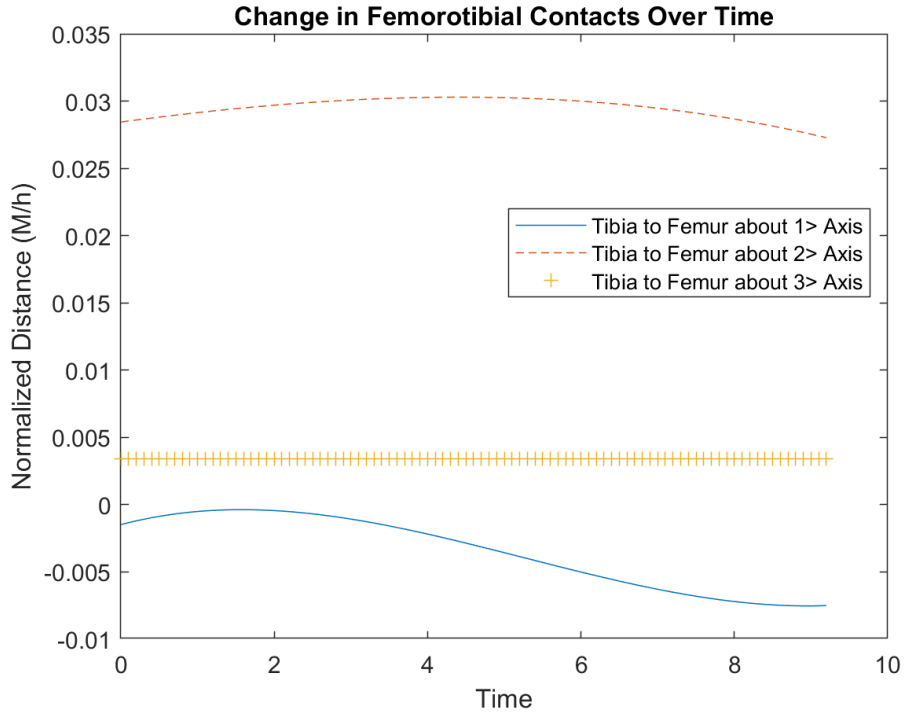

Figure 10: Plot showing tibia to femur about 1> axis, tibia to femur about 2> axis, and tibia to femur about 3> axis

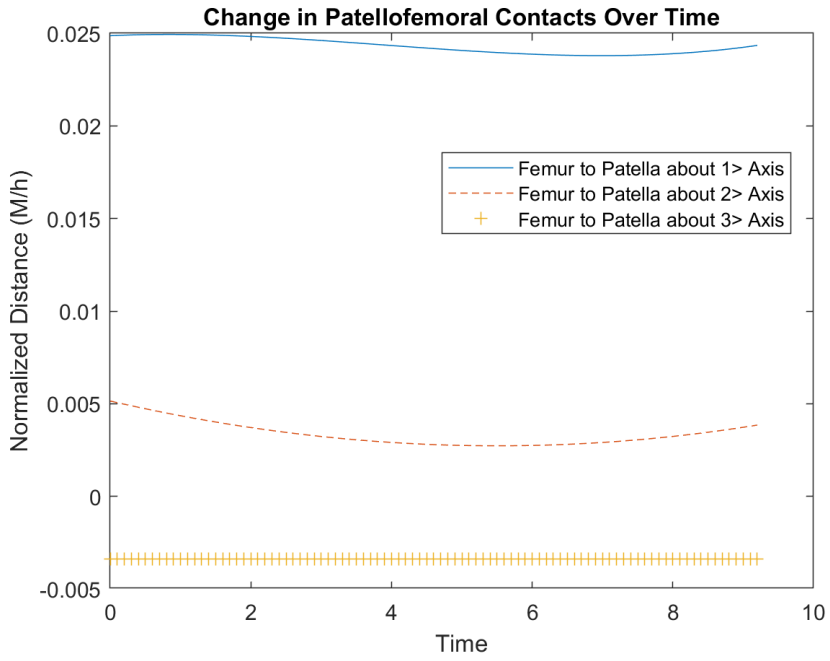

Figure 11: Plot showing femur to patella about 1> axis, femur to patella about 2> axis, & femur to patella about 3> axis

Model With Wrapping Figures

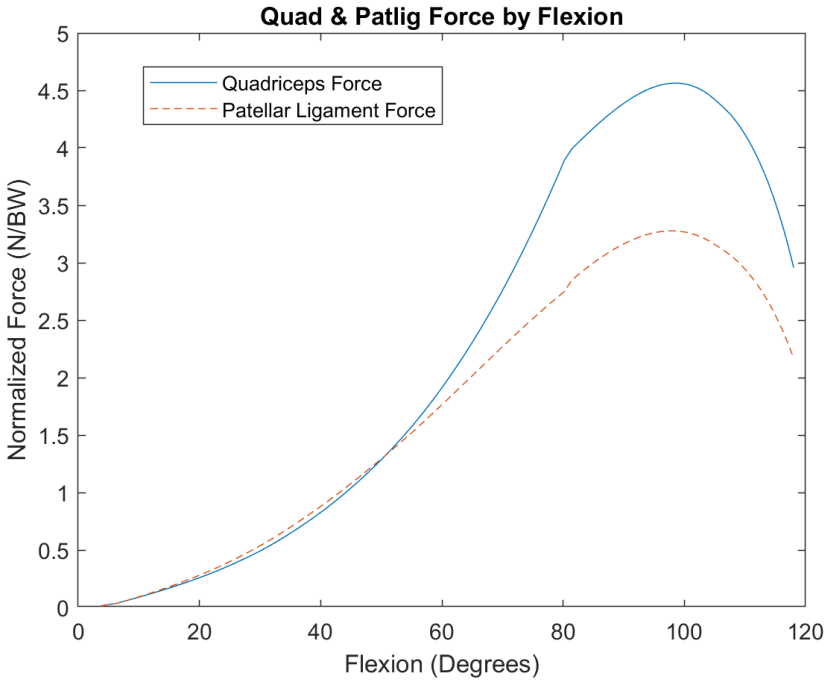

Figure 12: Plot showing the total quadriceps force and patellar ligament force

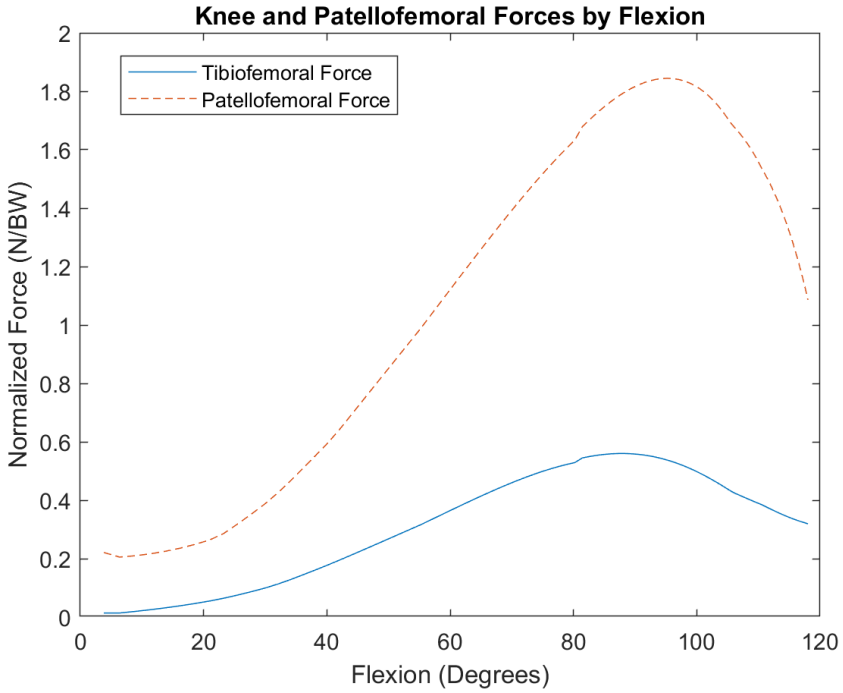

Figure 13: Plot showing the resultant tibiofemoral (knee) and patellofemoral forces

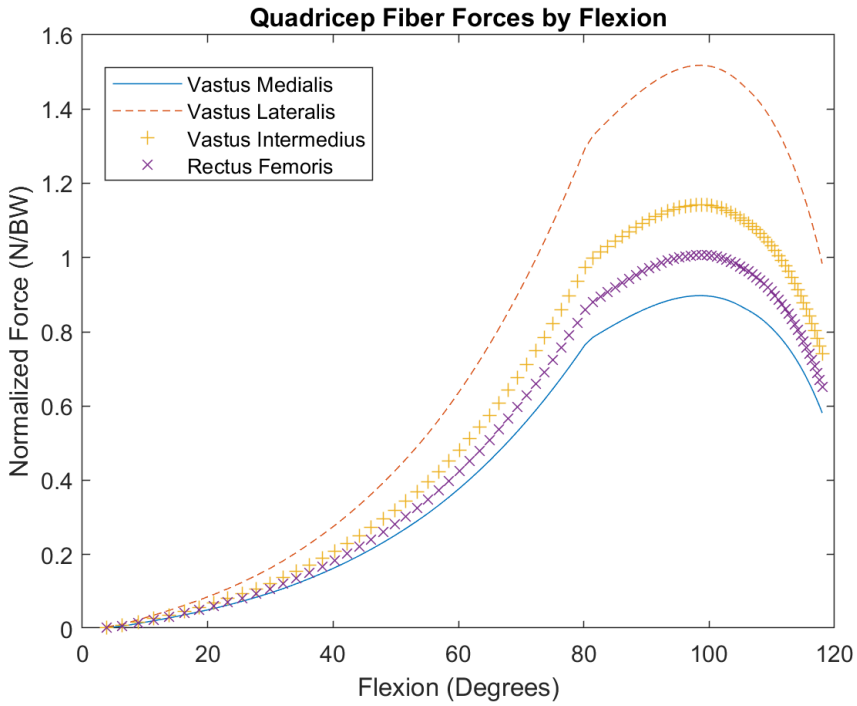

Figure 14: Plot showing the separate force in each quadriceps muscle fiber.

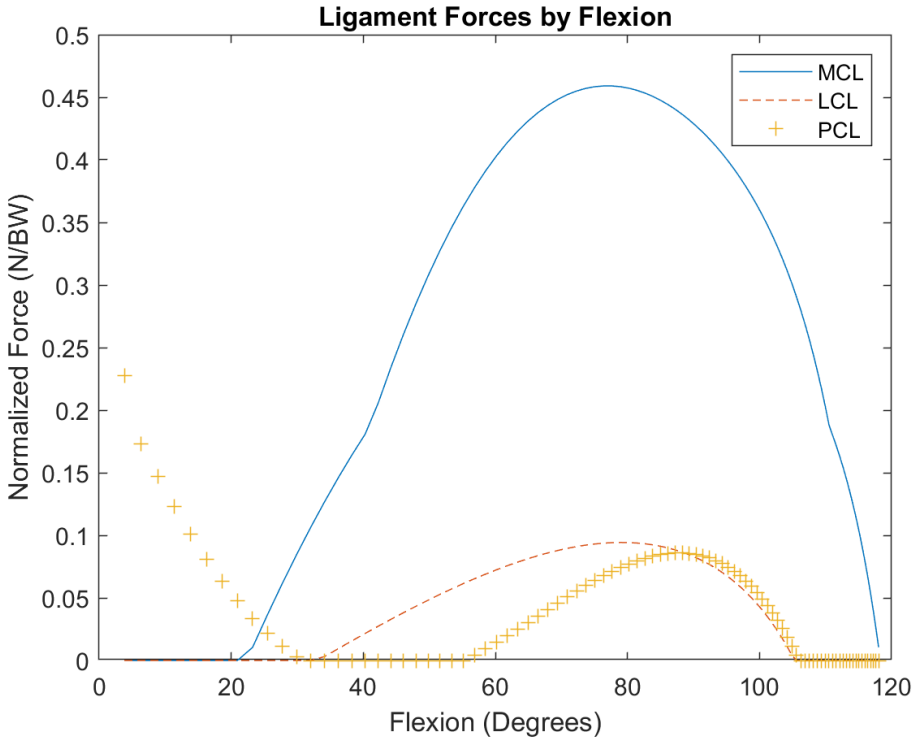

Figure 15: Plot showing the total MCL, LCL, and PCL ligament forces

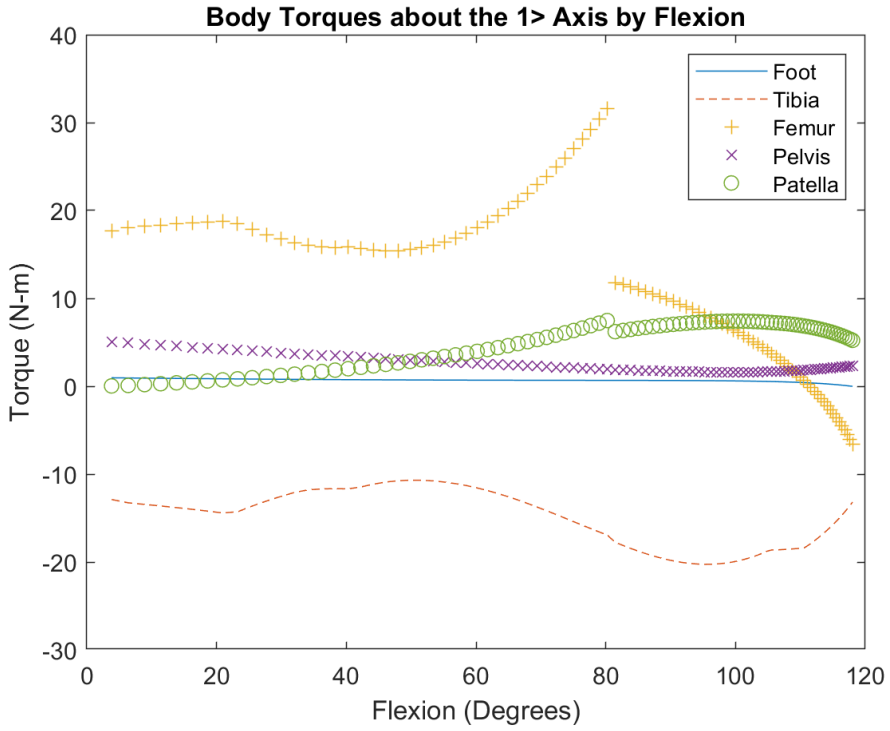

Figure 16: Plot showing the torques on the foot, tibia, femur, pelvis, and patella about the 1> axis

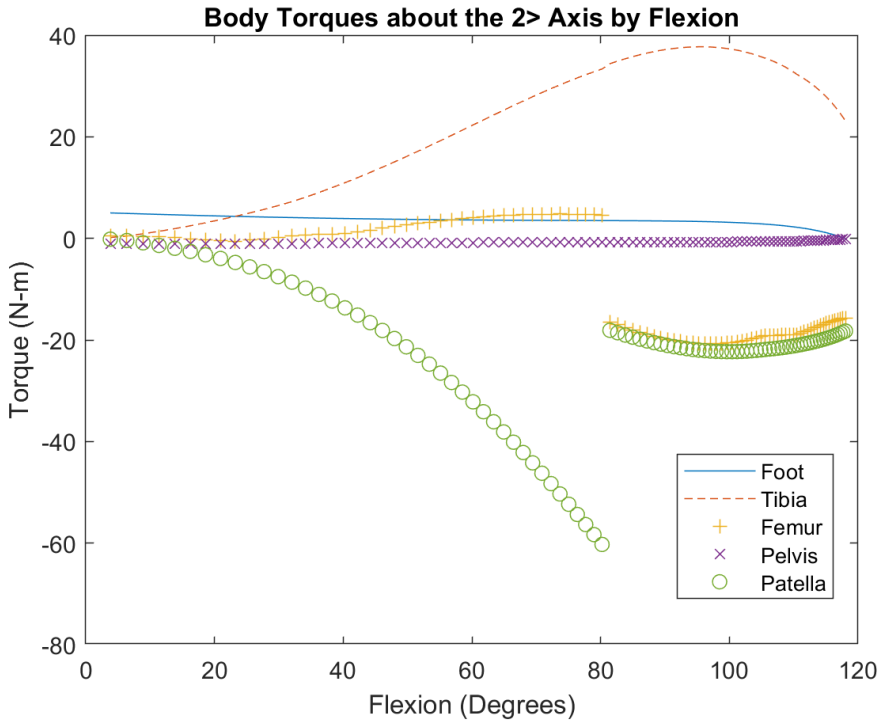

Figure 17: Plot showing the torques on the foot, tibia, femur, pelvis, and patella about the 2> axis

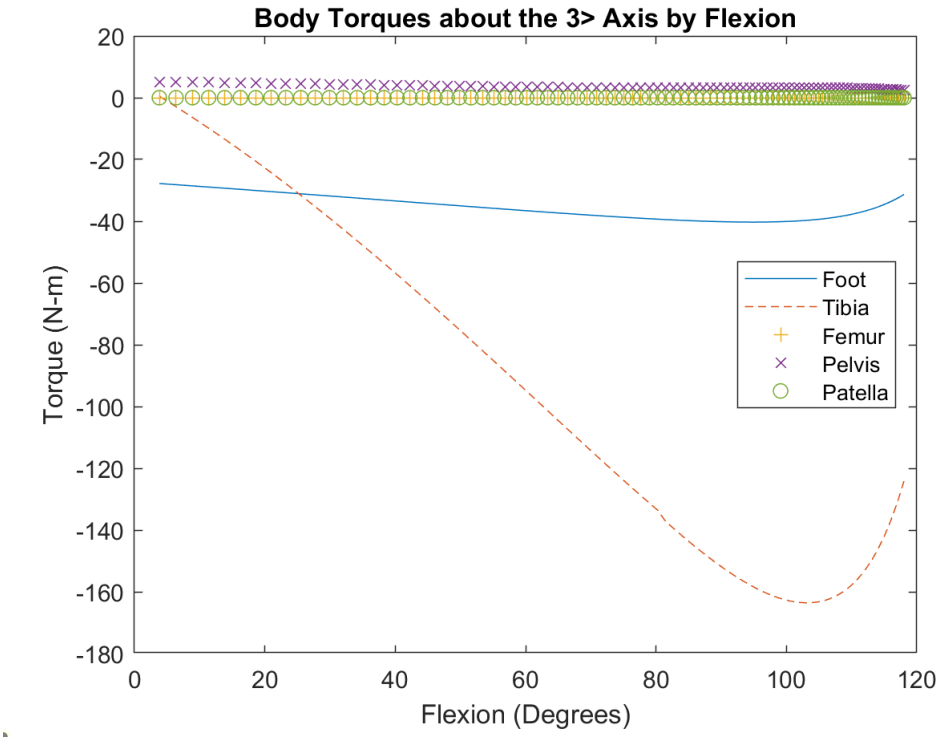

Figure 18: Plot showing the torques on the foot, tibia, femur, pelvis, and patella about the 3> axis

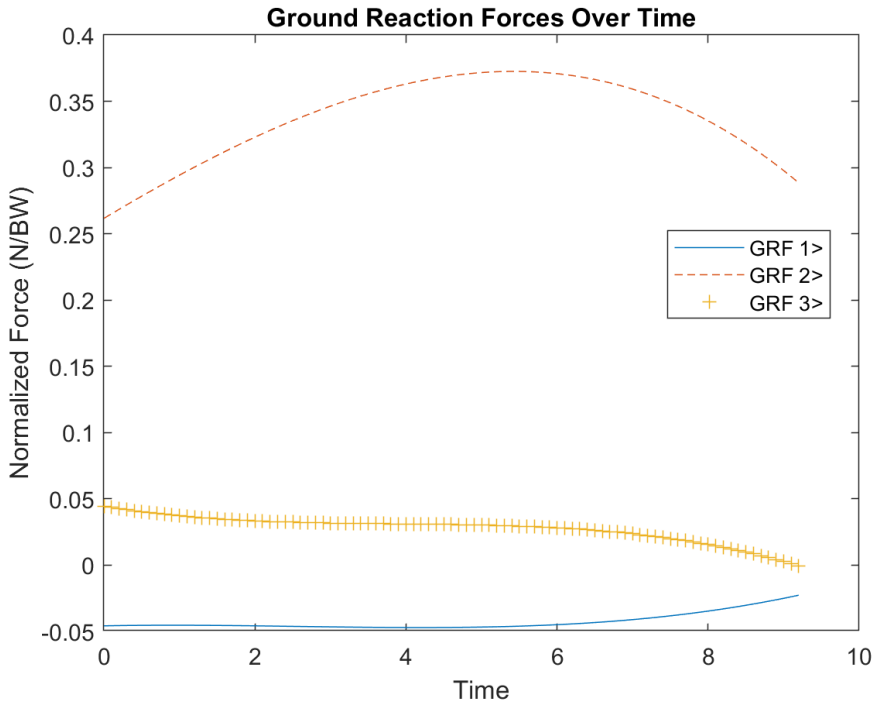

Figure 19: Plot showing the GRF forces in the 1>, 2>, and 3> direction

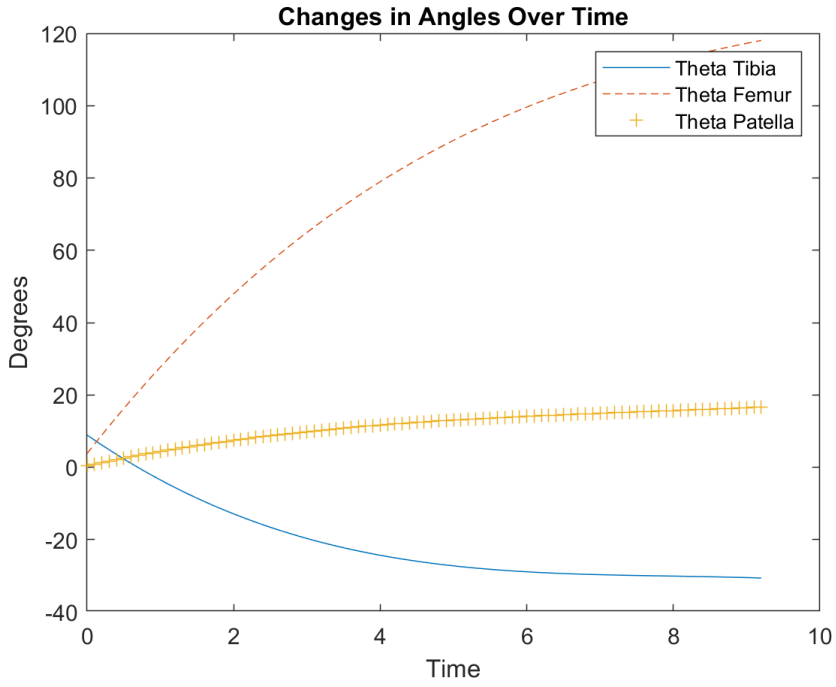

Figure 20: Plot showing theta tibia, theta femur about 3> axis , and theta patella about 3> axis

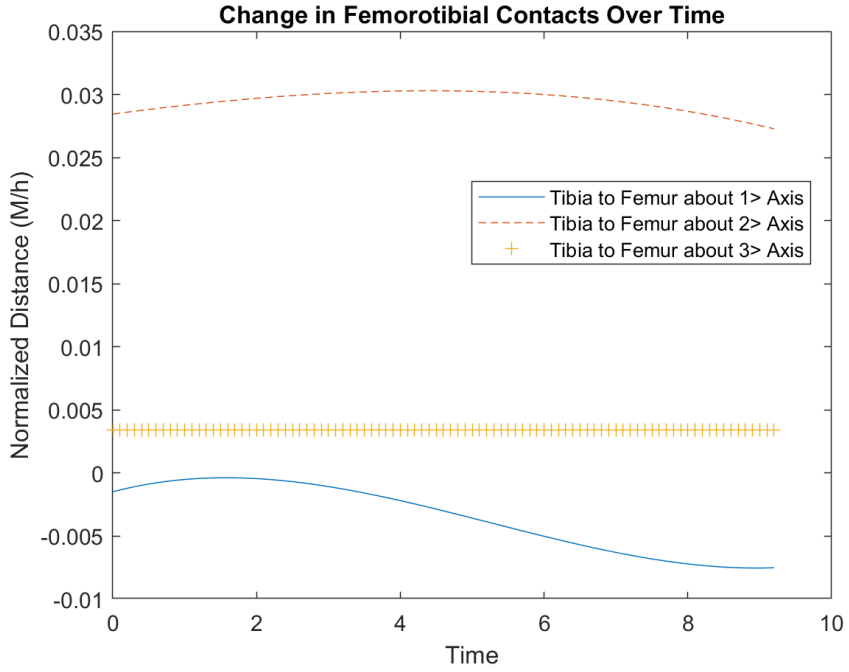

Figure 21: Plot showing tibia to femur about 1> axis, tibia to femur about 2> axis, and tibia to femur about 3> axis

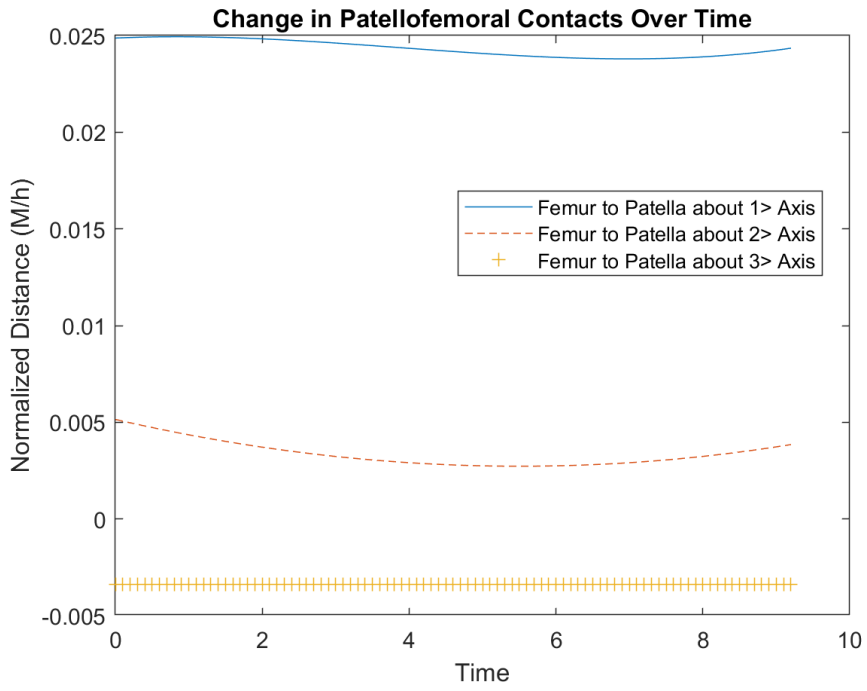

Figure 22: Plot showing femur to patella about 1> axis, femur to patella about 2> axis, & femur to patella about 3> axis